UNIVERSITY OF BUCHAREST

FACULTY OF CHEMISTRY
DOCTORAL SCHOOL IN CHEMISTRY

PhD THESIS
ABSTRACT

HETEROTRISPIN COMPLEXES

PhD Student:

Andrei-Alunel Pătrașcu

PhD Supervisor:

Acad. Marius Andruh

2025

The PhD thesis titled ”Heterotrispin Coordination Complexes” encompasses studies within the research fields of organic chemistry, coordination chemistry, crystal engineering, and molecular magnetism. Its main subject involves the synthesis and characterization of Mannich base-type ligands, stable nitronyl nitroxide radicals, and coordination compounds with three different spin carriers. Besides heterotrispin complexes, the thesis also includes heterobispin compounds.

The thesis consists of six chapters, two of which are literature reviews and four are original contributions. It presents 57 compounds, including 5 heterobinuclear 3*d*-4*f* complexes, 2 2*p*-3*d* complexes, 6 2*p*-4*f* complexes, 25 heterotrispin 2*p*-3*d*-4*f* complexes, and 19 heterotrimetallic 3*d*-4*f*-5*d* compounds.

1. The first literature chapter, ”Introduction to Stable Radicals Chemistry”, describes free organic radicals along with a brief classification. Stable organic radicals are of interest to chemists due to the presence of unpaired electrons. Radical-carrying molecules, which also include donor atoms like oxygen or nitrogen, are used in coordination chemistry in reactions with paramagnetic metal ions to create coordination complexes with interesting magnetic properties. Structurally and in terms of potential coordination modes, the stable radicals of interest in the mentioned fields include nitroxide, verdazyl, and nitronyl nitroxide (Scheme 1).

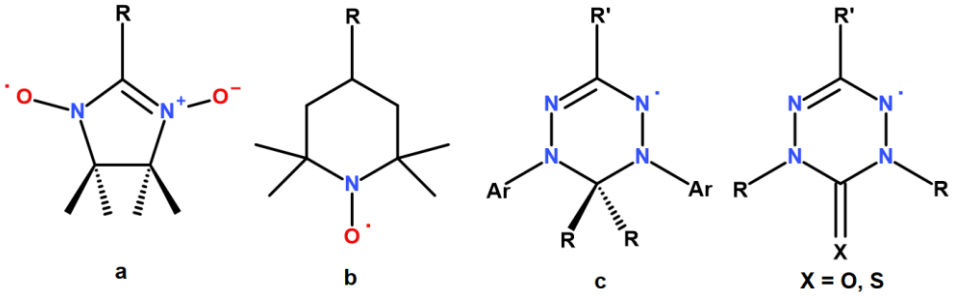

Scheme 1. Structures of nitronyl nitroxide radicals (a), TEMPO (b), and verdazyl (c).

2. In the second literature chapter, ”Heterotrispin 2*p*-3*d*-4*f* Coordination Complexes Derived from Organic Radicals”, stable organic radicals (TEMPO, verdazyl, $TCNQ^{\bullet-}$, and nitronyl nitroxide) are illustrated, which have significantly contributed to the development of molecular magnetism in 2*p*-3*d*-4*f* heterotrispin complex combinations. Paramagnetic ligands are essential due to their versatility in forming complex species with various metal ions. Magnetic ordering temperatures for purely organic magnets are low. Consequently, combining

them with metal ions (3*d*, 4*d*, and 4*f*) to improve magnetic performance is the most used strategy. However, this approach requires precise control of syntheses to ensure desired magnetic couplings and to fully understand magnetic interactions between spin carriers. These radicals can be decorated with various coordinating groups, and their structures allow different coordination modes, making them useful for creating coordination complexes with diverse topologies, nuclearities, and dimensionalities. This literature chapter describes discrete compounds, one-dimensional coordination polymers, as well as two-dimensional ones formed by stable organic radicals together with two different metal ions.

3. Chapter III, ”Precursors for Obtaining 2*p*-3*d*-4*f* Systems”, part of the original contributions, presents: i) the development of a synthesis strategy for heterometallic 3*d*-4*f* coordination polymers using the node-and-spacer approach; ii) the synthesis of two 2*p*-3*d*-4*f* compounds using a heterobimetallic precursor containing an easily substitutable acetato group (Scheme 2).

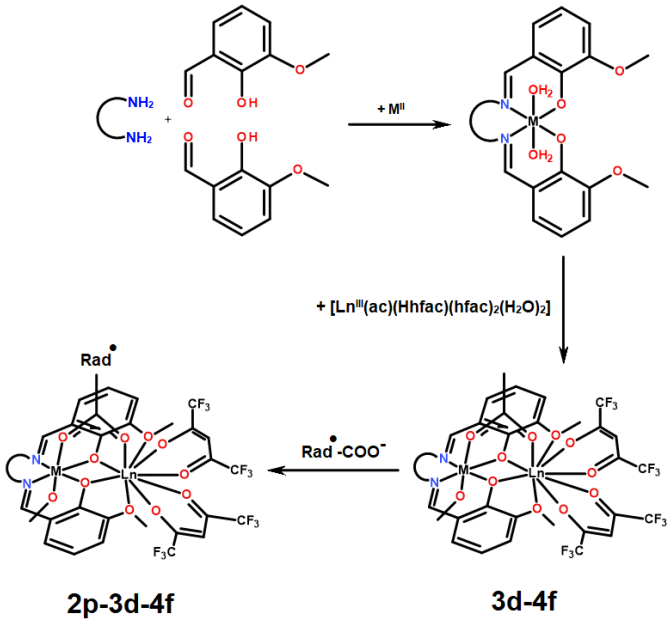

Scheme 2. The reaction scheme for obtaining 2*p*-3*d*-4*f* derivatives using 3*d*-4*f* complex combinations and anionic radicals.

Replacing the acetato ligand with other anionic ligands containing a carboxylate group (isonicotinate anion and the 4-carboxy-TEMPO radical anion, respectively) represents a promising synthesis method for new molecular magnetic systems. The ability of the acetato ligand to be easily replaced and to form extended structures was demonstrated using

isonicotinic acid as a spacer. Four new one-dimensional coordination polymers were obtained ($^{1}_{\infty}$[Co(valpn)Gd(hfac)$_2$(IN)] **1**, $^{1}_{\infty}$[Ni(valpn)Gd(hfac)$_2$(IN)] **2**, $^{1}_{\infty}$[Ni(valpn)Dy(hfac)$_2$(IN)] **3**, and $^{1}_{\infty}$[Ni(valpn)Pr(hfac)$_2$(IN)] **4**), as well as one oligonuclear compound, [Zn(valpn)Eu(hfac)$_2$(IN)] **5**.

The synthesis of compounds of the type [M(valpn)Ln(hfac)$_2$(IN)] was carried out by forming the Schiff base-type ligand in the first step, followed by the complexation of 3*d* and 4*f* metal ions, and completed by the addition of deprotonated isonicotinic acid with triethylamine. In the case of the Co^{II} ion, the procedure was optimized by omitting the deprotonation of the Schiff base ligand, thus preventing its oxidation to Co^{III} under basic conditions.

The Ni^{II} isostructural compounds (**2**, **3**, and **4**) exhibit structural similarities to the Co^{II} compound **1**. The main differences lie in the orientation of the axes of the dinuclear nodes, which influence the resulting topology. Thus, compound **1** has a linear chain structure, while compounds **2** - **4** have a zigzag structure (Figure 1). The 3*d*-4*f* dinuclear nodes are interconnected through isonicotinato anionic spacers. Each spacer of this type forms *syn-syn* bridges via the carboxylato group, which binds the metal ions within the same dinuclear unit. Additionally, the pyridinic nitrogen atom coordinates with the cobalt/nickel ion within an adjacent dinuclear unit, thereby forming the coordination polymer.

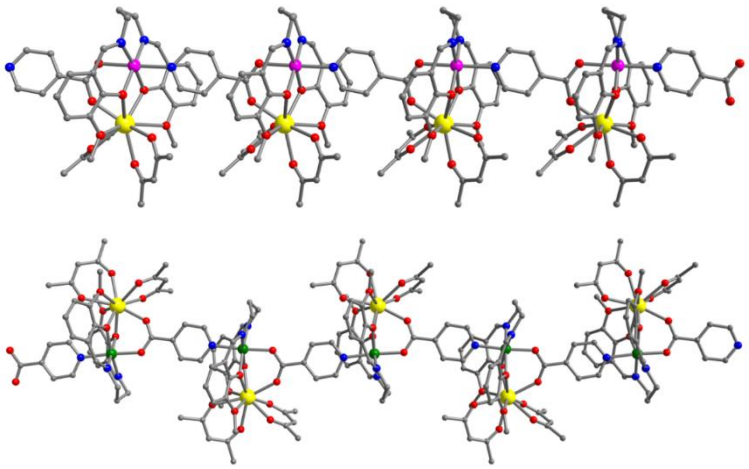

Figure 1. The structures of chains **1** (top) and **2** - **4** (bottom).

The AC magnetic susceptibility measurements of compound **3** indicate a weak frequency dependence of the AC susceptibility at low temperatures under an applied external field of 1 kOe, which corresponds to the slow relaxation of magnetization, characteristic of an SMM (Figure 2). For compounds **1** and **2**, no frequency dependence was observed at low

temperatures, neither in the absence of an external magnetic field nor under an applied field of 1 kOe. Compound **3** behaves as a chain in which the dinuclear nodes exhibit SMM properties.

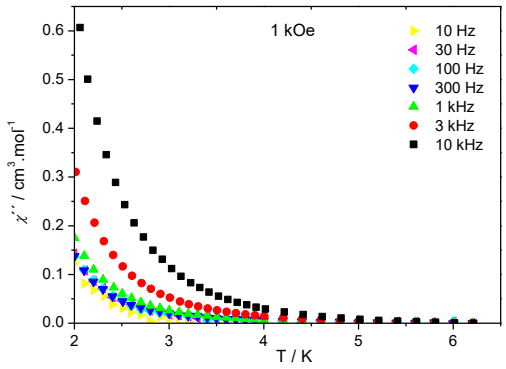

Figure 2. The temperature dependence of the out-of-phase (χ") susceptibility component for compound **3** under an external field (H_{ext}) of 1 kOe, at different frequencies of the magnetic field.

The structure of the complex [Zn(valpn)Eu(hfac)$_2$(IN)] **5** consists of two different units within the asymmetric unit, which differ in the nature of the spacer, stabilized through cocrystallization and having the molecular formula [Zn(valpn)Eu(hfac)$_2$(IN)][Zn(valpn)Eu(hfac)$_2$(ac)]. The first unit features the isonicotinato anion as a bridge between the two metal ions, while the second unit features the acetato anion as the bridge.

Two new heterotrispin compounds were obtained: [Ni(valpn)Pr(hfac)$_2$(4-carboxy-TEMPO)] **6** and [Ni(valpn)Gd(hfac)$_2$(4-carboxy-TEMPO)] **7**, in which the Ni^{II} and Gd^{III} ions are connected via the carboxylate bridge of the 4-carboxy-TEMPO radical and phenoxido bridges (Figure 3). The distances between the organic radical and the two metal ions are relatively large (Ni1 - N3 = 7.144(8) Å and Gd1 - N3 = 6.959(8) Å, respectively), indicating magnetic isolation of the 2*p* electron from the two paramagnetic metal ions.

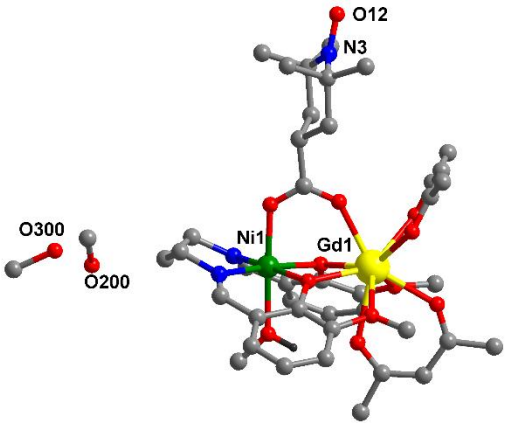

Figure 3. The structural representation of the compound [Ni(valpn)Gd(hfac)$_2$(4-carboxy-TEMPO)] **7**.

4. Chapter IV, ”Oligonuclear 2*p*-3*d*-4*f* Compounds Constructed Using Compartmental Nitronyl Nitroxide Organic Radicals”, illustrates the synthesis and characterization of oligonuclear 2*p*-3*d*, 2*p*-4*f*, and 2*p*-3*d*-4*f* compounds. These were obtained using an asymmetric compartmental nitronyl nitroxide organic radical (HL), which is based on a Mannich base containing an arm derived from N,N,N’-trimethylethylenediamine (Scheme 3). This radical shows a clear selectivity for metal ions, tailored to accommodate both 3*d* and 4*f* ions.

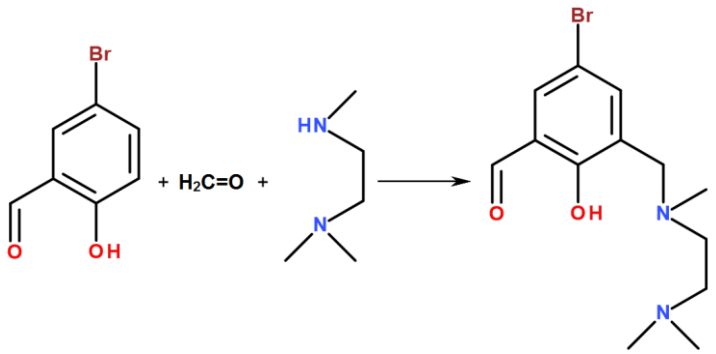

Scheme 3. The reaction scheme of the compartmental Mannich base.

The use of compartmental nitronyl nitroxide radicals (Scheme 4) represents a new strategy for obtaining predictable structures capable of generating strong magnetic interactions between all spin carriers. To validate the coordinating behavior of the bicompartmental nitronyl nitroxide radical, a series of experiments were conducted in which the radical was reacted separately with different types of precursors: $[Ln(hfac)_3(H_2O)_2]$, $[M^{II}(hfac)_2(H_2O)_2]$, as well as an equimolar mixture of these. The bicompartmental radical demonstrated a high selectivity in its interactions with different metal ions: the OO’ compartment was suitable for oxophilic lanthanide ions, while the ONN’ compartment was optimal for transition metal ions.

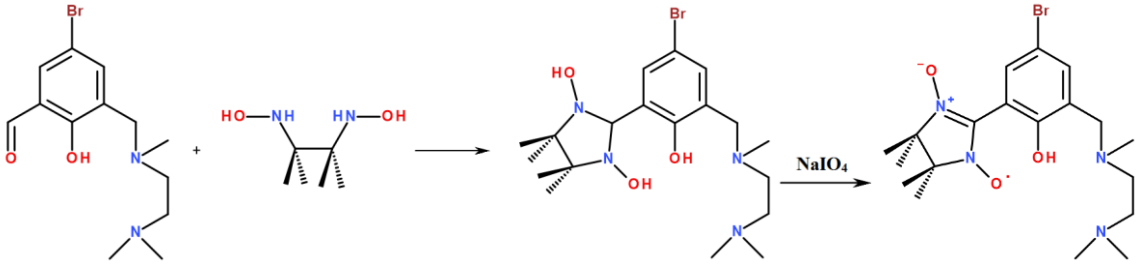

Scheme 4. The synthesis scheme of the compartmental nitronyl nitroxide radical HL.

Three main classes of compounds have been synthesized (Figure 4):

i. 2*p*-4*f* complexes: [Tb(LH)(hfac)$_3$] **8** and [Dy(LH)(hfac)$_3$] **9**, with the oxophilic Ln^{III} ion located in the {OO'} compartment, which consists of a phenoxido oxygen atom and an oxygen atom originating from an aminoxyl group of the radical. The {ONN'} compartment is not involved in coordination;

ii. 2*p*-3*d* complexes: [Mn_2L(hfac)$_3$] **10** and [Co_2L(hfac)$_3$] **11**, which demonstrated that 3*d* metal ions can occupy both compartments of the ligand, {OO'} and {ONN'}, without a clear preference for nitrogen or oxygen atoms;

iii. 2*p*-3*d*-4*f* complexes: [CoGdL(hfac)$_4$] **12**, [CoTbL(hfac)$_4$] **13**, and [CoDyL(hfac)$_4$] **14**, with the 3*d* metal ion located in the first compartment {ONN'} and the 4*f* ion in the second compartment {OO'}.

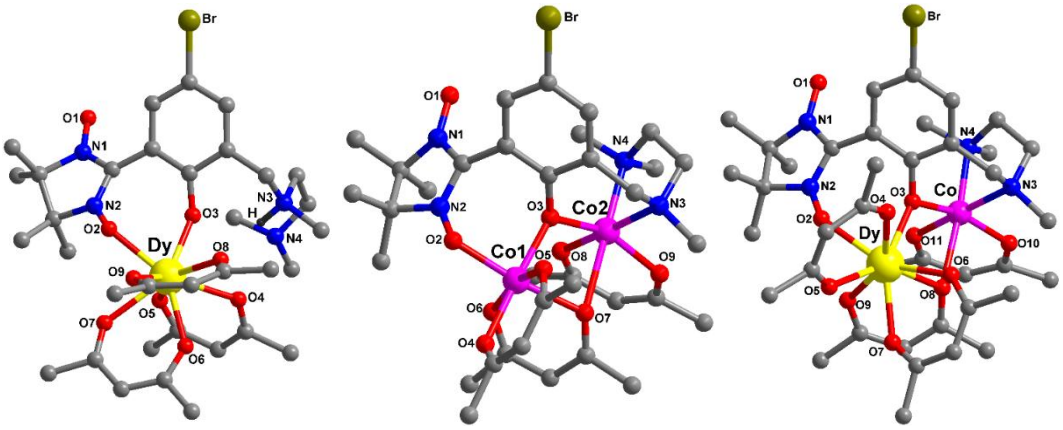

Figure 4. The molecular structure of the compounds [Dy(LH)(hfac)$_3$] **9**, [Co_2L(hfac)$_3$] **11**, and [CoDyL(hfac)$_4$] **14**.

The magnetic behavior of the compound [Dy(LH)(hfac)$_3$] **9** indicates the presence of a ferromagnetic interaction between the Dy^{III} ion and the organic radical. This is evidenced by the increase in the $\chi_M T$ product value at low temperatures (below 45 K). The Dy^{III} ion exhibits strong axial anisotropy, with a high *g* component value along the principal axis (g_z = 19.2). The first excited state is well-separated from the ground state (112 cm^{-1}), suggesting magnetic stability and the potential for single-ion magnet (SIM) behavior.

The dynamic magnetic properties highlighted through AC susceptibility measurements showed slow magnetization relaxation for the compound [Dy(LH)(hfac)$_3$] **9**. At low temperatures and zero magnetic field, the phenomenon of quantum tunneling of magnetization was observed. This behavior was suppressed by applying an external magnetic field (H = 1 kOe) (Figure 5).

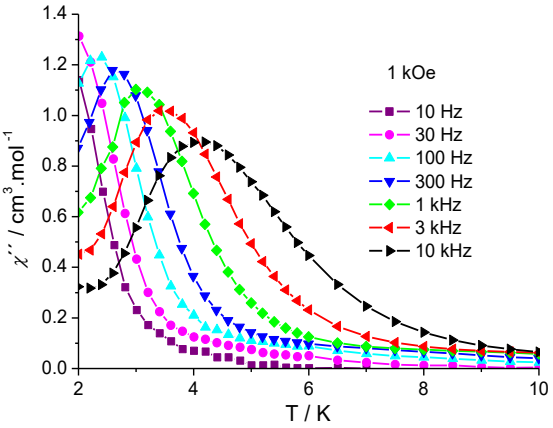

Figure 5. The temperature dependence of the out-of-phase component of susceptibility (χ") for the compound [Dy(LH)(hfac)$_3$] **9** measured under the influence of an applied external field H = 1 kOe.

The organic radical in the compound [CoDyL(hfac)$_4$] **14** interacts ferromagnetically with the Dy^{III} and Co^{II} ions, with the values: J_{DyRad} = 0.78 cm^{-1} and J_{CoRad} = 0.12 cm^{-1}. The interaction between Dy^{III} and Co^{II} is antiferromagnetic, with J_{CoDy} = -2.0 cm^{-1}.

Unlike the compound [Dy(LH)(hfac)$_3$] **9**, the compound [CoDyL(hfac)$_4$] **14** does not exhibit frequency dependence of AC magnetic susceptibility under zero static magnetic field. Under a non-zero external field (H = 1.5 kOe), a weak frequency dependence appears, indicating weak SMM behavior (Figure 6). The magnetization axes of the Dy^{III} and Co^{II} ions are tilted at an angle of 63°, which may explain the observed magnetic behavior.

The compound [CoDyL(hfac)$_4$] **14** represents a successful example of directed synthesis for new heterotrispin complexes with predictable structures, although the observed magnetic properties did not reach the desired level.

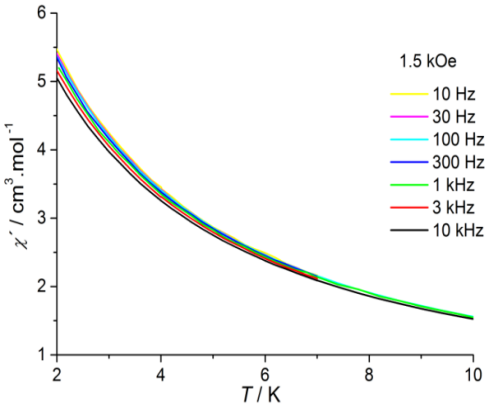

Figure 6. The temperature dependence of the in-phase component of susceptibility (χ') for the compound [CoDyL(hfac)$_4$] **14** under an external field H_{ext} = 1.5 kOe.

5. Chapter V, "The First 2*p*-3*d*-4*f* Heterospin Compounds with Different Metal Ions Connected via an Aminoxyl Group", presents the results on the use of asymmetric compartmental nitronyl nitroxide radicals, in which the amines forming the arm of the Mannich base contain a single nitrogen atom (HL^1, HL^2, HL^3, *S*-HL^4 și *R*-HL^4) (Scheme 5). This allowed for changes in the arrangement of spin carriers and their interactions compared to the compounds described in Chapter **IV**.

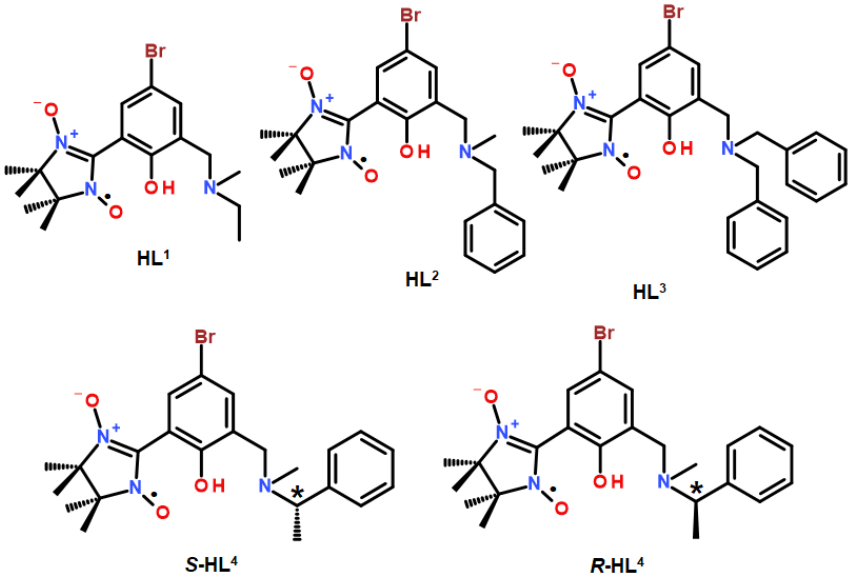

Scheme 5. The schemes of the asymmetric nitronyl nitroxide radicals obtained.

The use of new compartmental radicals led to the synthesis of 22 new compounds. The resulting complexes include various combinations of Co, Mn, Ni, and Zn metal ions with lanthanides Gd, Tb, Dy, and Y, allowing for detailed exploration of their magnetic behavior. An important feature observed in all heterospin compounds is the proton transfer from the phenolic group to the nitrogen atom of the amine group. Thus, the amine arm of the Mannich base is not involved in the coordination to metal ions. Also relevant in this case is the fact that both M^{II} and Ln^{III} ions coordinate to the same oxygen atom of the radical.

The 2*p*-3*d*-4*f* compounds described in this chapter are the first examples in which the aminoxyl group functions as a bridge presenting an unpaired electron between two different metal ions (Figure 7). More precisely, the three different spin carriers interact directly, without the need for an additional auxiliary bridge.

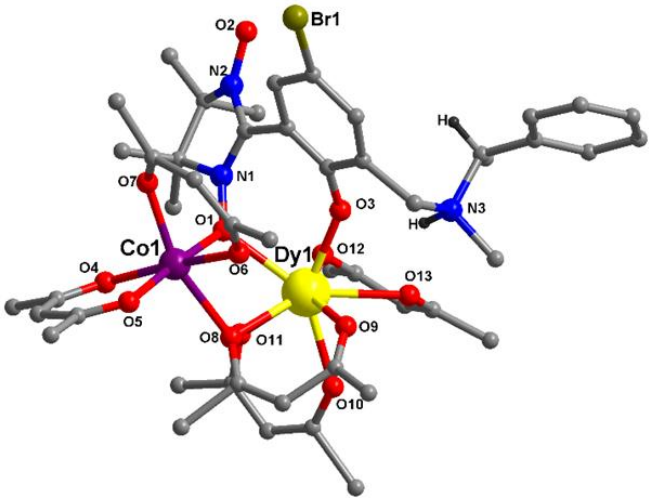

Figure 7. The structural representation of a crystallographically independent binuclear unit of compound **33**.

Of all the synthesized compounds, three 2*p*-4*f* compounds were obtained: [Dy(L^2H)(hfac)$_3$] **18**, [Dy(L^3H)(hfac)$_3$] **20**, and [Dy(*R*-L^4H)(hfac)$_5$] **31** (Figure 8). The synthesis of any 2*p*-3*d* compound was not successful. This observation may indicate a certain selectivity of nitronyl nitroxide radicals for 4*f* ions compared to 3*d* ions.

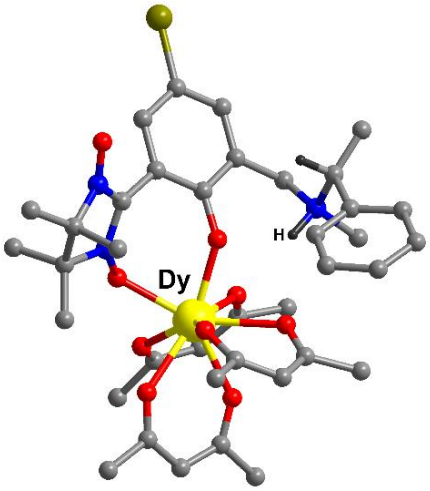

Figure 8. The structure of the chiral mononuclear compound [Dy(*R*-L^4H)(hfac)$_5$] **31**.

In the chiral compound **33**, examining both independent units in the crystal, it is observed that in one unit, the amino nitrogen atom becomes chiral through protonation, presenting the *R* configuration, while in the other unit, it has the *S* configuration. Both the Co^{II} and Dy^{III} ions are chiral. Within one unit, the centers N3, Co1, and Dy1 exhibit the configurations *S*, *Λ*, and *Δ* (**33**$_{(SΛΔ)}$), while in the other unit, the centers N6, Co2, and Dy2

exhibit the configurations *R*, *Λ*, and *Δ* (**33**$_{(RΛΔ)}$). This indicates that two diastereoisomers are present in the crystal of compound **33** (Figure 9).

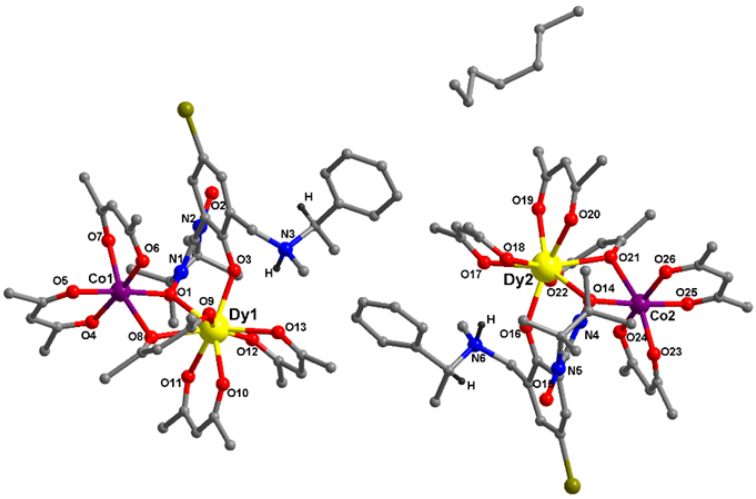

Figure 9. The structural representation of the two independent binuclear units in the crystal of compound [CoDy(*R*-L^{4}H)(hfac)$_5$] **33**.

The enantiomeric nature of the two crystals [CoDy(*R*-L^{4}H)(hfac)$_5$] **33** and [CoDy(*S*-L^{4}H)(hfac)$_5$] **25** was demonstrated through solid-state circular dichroism spectroscopy (Figure 10).

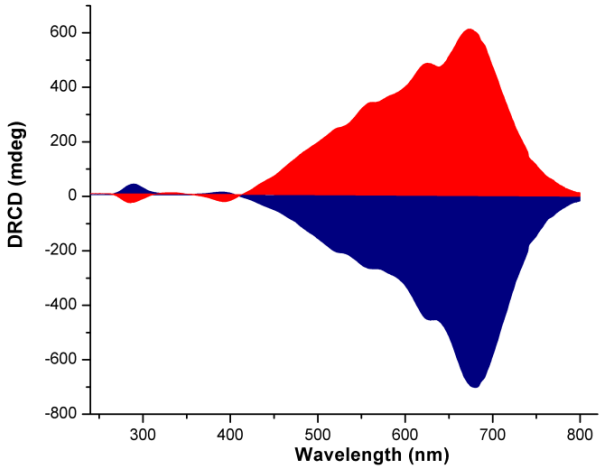

Figure 10. The solid-state circular dichroism spectrum for **33** (blue) and **25** (red).

The magnetic properties of the compounds [CoGd(*R*-L^{4}H)(hfac)$_5$] **32**, [CoDy(*R*-L^{4}H)(hfac)$_5$] **33**, and [ZnDy(*S*-L^{4}H)(hfac)$_5$] **30** were investigated between 2 and 300 K to analyze the influence of the 3*d* metal ion. The replacement of the paramagnetic Co^{II} ion with the diamagnetic Zn^{II} ion eliminated the 2*p*-3*d* and 3*d*-4*f* coupling pathways.

For the compound [CoDy(*R*-L^{4}H)(hfac)$_5$] **33**, the decrease in the $\chi_M T$ product value at high temperatures originates from the intrinsic magnetism of the Dy^{III} ion (depopulation of the M_J sublevels of the $^6H_{15/2}$ ground state) and from the magnetic anisotropy (spin-orbit coupling) of the Co^{II} ion (Figure 10). DC magnetic susceptibility measurements performed on compound **25** showed a superimposable behavior with that of enantiomer **33**.

In the case of the compound [ZnDy(*S*-L^{4}H)(hfac)$_5$] **30**, the intrinsic magnetism of the Dy^{III} ion is involved. However, at very low temperatures, a ferromagnetic interaction between the Nit and Dy^{III} is observed (Figure 10).

In the compound [CoGd(*R*-L^{4}H)(hfac)$_5$] **32**, the decrease in the $\chi_M T$ product value as the temperature drops indicates an antiferromagnetic interaction between Nit and Co^{II}, followed by an increase, which suggests ferromagnetic exchange interactions for the other couplings (Nit-Gd^{III} and Co^{II}-Gd^{III}) (Figure 10).

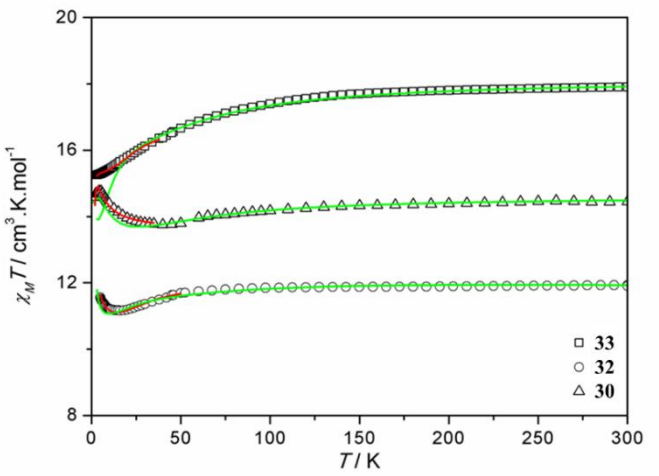

Figure 10. The $\chi_M T$ vs. T data for the compounds [CoDy(*R*-L^{4}H)(hfac)$_5$] **33**, [CoGd(*R*-L^{4}H)(hfac)$_5$] **32**, and [ZnDy(*S*-L^{4}H)(hfac)$_5$] **30**.

The complex [CoDy(*R*-L^{4}H)(hfac)$_5$] **33** has a blocking temperature of 28 K, which is high among heterospin compounds (Figure 11). The compound [ZnDy(*S*-L^{4}H)(hfac)$_5$] **30** exhibits SMM behavior at 17 K, which represents a normal to slightly elevated temperature compared to most SMMs studied in the literature (Figure 12). The comparison of the magnetic behavior of compounds **30** and **33** clearly highlighted the synergy of the three coupling pathways (2*p*-3*d*, 3*d*-4*f*, and 2*p*-4*f*), which led to higher performance of the complex combinations exhibiting SMM behavior.

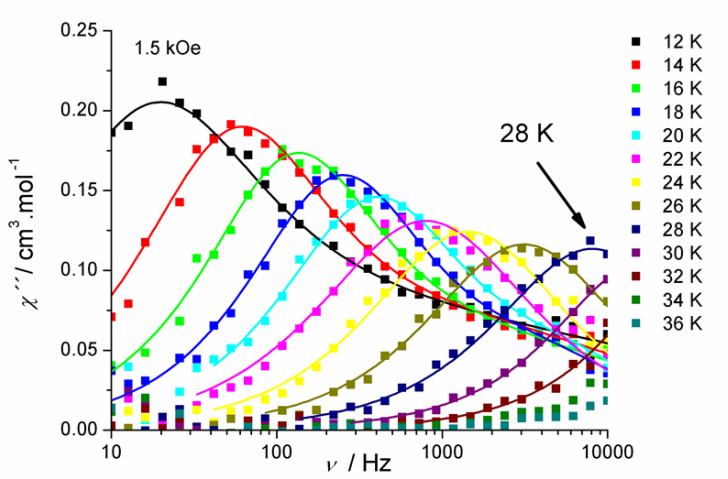

Figure 11. The frequency dependence at different temperatures of the out-of-phase magnetic susceptibility (χ") under the influence of an external field of H_{dc} = 1500 Oe for compound **33**.

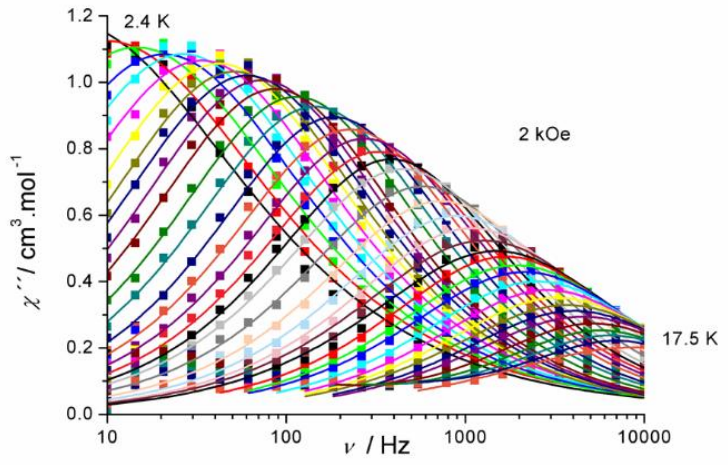

Figure 12. The frequency dependence at different temperatures of the out-of-phase magnetic susceptibility (χ") under the influence of an external field of H_{dc} = 2000 Oe for compound **30**.

Comparing the compound [CoDy(*R*-L^4H)(hfac)$_5$] **33** cu [CoDyL(hfac)$_4$] **14** reveals significant differences in spin topology and exchange coupling pathways. While [CoDyL(hfac)$_4$] **14** has a linear topology with weak Nit-Co^{II} interactions, the compound [CoDy(*R*-L^4H)(hfac)$_5$] **33** exhibits a triangular topology with simultaneous interactions between Nit-M^{II}, Nit-Ln^{III}, and M^{II}-Ln^{III}. Additionally, the most important difference between the two complexes is the nitroxide bridge in compound **33**, which mediates direct interactions between the three different spin carriers.

6. Continuing our focus on heterotrispin molecular magnetic systems, we also aimed to synthesize heterotrimetallic compounds. Chapter VI, "Heterotrimetallic 3*d*-4*f*-5*d* Complexes Derived from Re^{IV} as a Metalloligand. Preliminary Results", illustrates the coordination ability of an Re^{IV} metalloligand, specifically $[ReBr_5(3,5\text{-pydc})]^{3-}$ (3,5-pydc - the dianion of 3,5-pyridinedicarboxylic acid) (Figure 13). These represent the only 3*d*-4*f*-5*d* heterotrimetallic compounds containing Re^{IV} ions. Four series of 3*d*-4*f*-5*d* complex combinations were synthesized and characterized by single-crystal X-ray diffraction. The study demonstrated that the metalloligand can efficiently coordinate, via carboxylate groups, to both 3*d* metal ions (Co^{II}, Ni^{II}, Cu^{II}, Zn^{II}) and lanthanide ions (Ln^{III}) within binuclear units of the type $[M(valpn)Ln]^{3+}$. The magnetic properties of the obtained compounds are to be investigated and analyzed in the future.

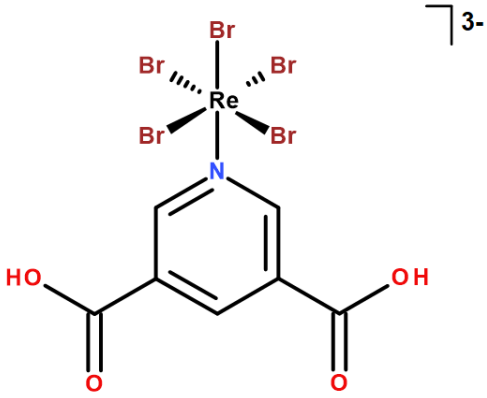

Figure 13. The representation of the metalloligand $[ReBr_5(3,5\text{-pydc})]^{3-}$.

Depending on the reaction conditions and the nature of the binuclear precursors used, several types of coordination architectures were obtained:

i. Hexanuclear Complexes of Type 1: Five complexes were obtained (Figure 14). These are characterized by a planar structure in which two binuclear M^{II}-Ln^{III} units are linked by two metalloligand units of $[ReBr_5(3,5\text{-pydc})]^{3-}$. A carboxylato group of the metalloligand coordinates as a bridging *syn-syn* ligand to both the M^{II} ion and the Ln^{III} ion, while the second carboxylato group coordinates only to the Ln^{III} ion through a single oxygen atom. This type of arrangement was observed for hexacoordinated 3*d* metal ions, such as Co^{II} and Ni^{II}.

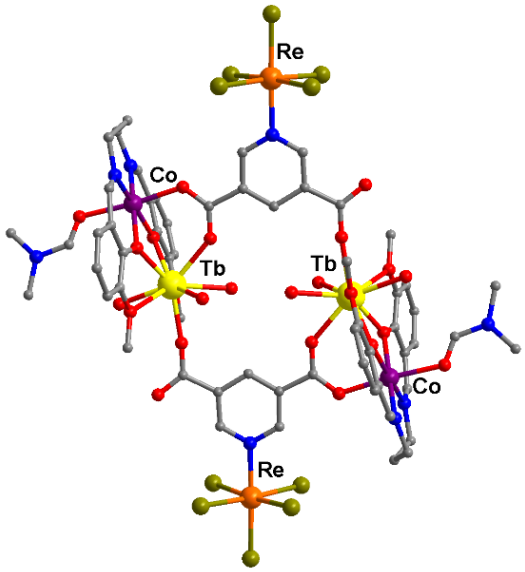

Figure 14. The structural representation of the compound [{$ReBr_5$(3,5-pydc)}$_2${Co(valpn)(DMF)Tb(H_2O)$_3$}$_2$] **40**.

ii. Hexanuclear Complexes of Type 2: Two complexes were obtained (Figure 15). The major difference compared to Type 1 lies in the ”V”-shaped arrangement of the binuclear units and the metalloligands, resulting from the use of pentacoordinated 3*d* metal ions, Cu^{II} and Zn^{II}. A carboxylato group acts as a *syn-syn* bridging ligand between the two metal ions of the 3*d*-4*f* binuclear precursor, while the second carboxylato group coordinates terminally through a single oxygen atom to the oxophilic Ln^{III} ion.

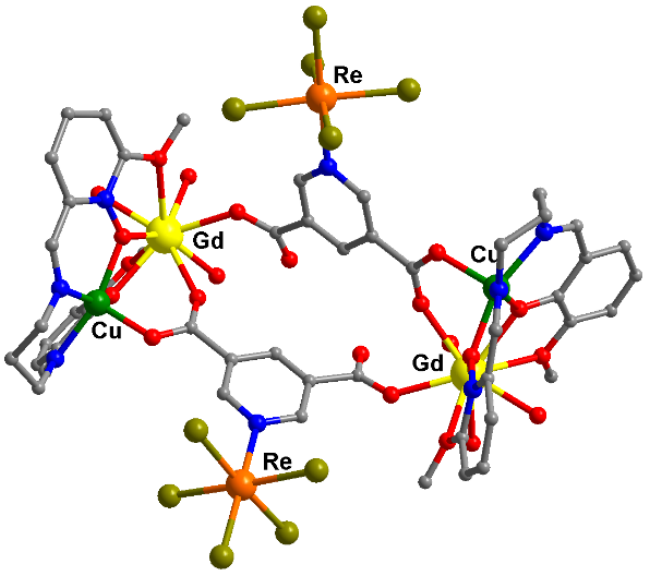

Figure 15. The structural representation of the compound [{$ReBr_5$(3,5-pydc)}$_2${Cu(valpn)Gd(H_2O)$_3$}$_2$] **44**.

iii. One-Dimensional Coordination Polymers of Type 1: Six chains were obtained (Figure 16). These linear structures consist of M^{II}-Ln^{III} binuclear units and $[ReBr_5(3,5\text{-pydc})]^{3-}$ units arranged in a zigzag pattern, acting as bridging ligands. The metalloligand $[ReBr_5(3,5\text{-pydc})]^{3-}$ coordinates via its two deprotonated carboxylato groups to both the M^{II} and Ln^{III} metal ions. Both carboxylato groups act as *syn-syn* bridging ligands between the two metal ions of the 3*d*-4*f* binuclear precursor. The type of coordination polymer depends on the coordination geometry of the 3*d* metal ions, specifically the hexacoordinated Co^{II} and Ni^{II}.

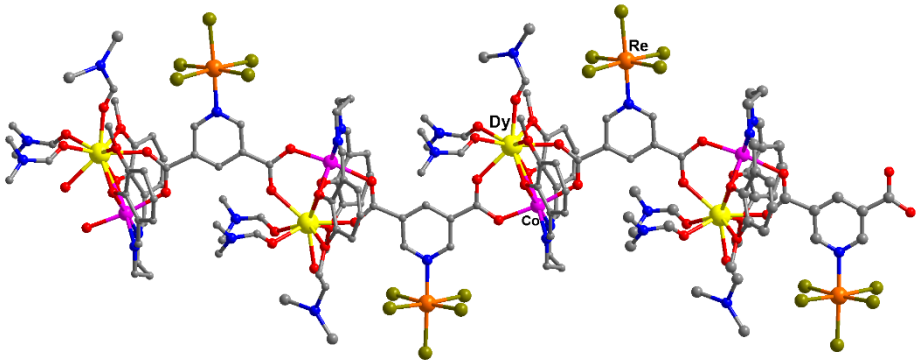

Figure 16. The structural representation of the compound $^{1}_{\infty}[\{ReBr_5(3,5\text{-pydc})\}_2\{Co(valpn)Dy(DMF)_3\}_2]$ **48**.

iv. One-Dimensional Coordination Polymers of Type 2: Six chains were obtained (Figure 17). The metalloligand $[ReBr_5(3,5\text{-pydc})]^{3-}$ coordinates via its two deprotonated carboxylato groups to both the M^{II} and Ln^{III} metal ions. One carboxylato group acts as a *syn-syn* bridging ligand between the two metal ions of the 3*d*-4*f* binuclear precursor. The second carboxylato group coordinates via a single oxygen atom to the Ln^{III} ion originating from an adjacent M^{II}-Ln^{III} binuclear unit. This type of arrangement was observed for pentacoordinated 3*d* metal ions such as Cu^{II} and Zn^{II}.

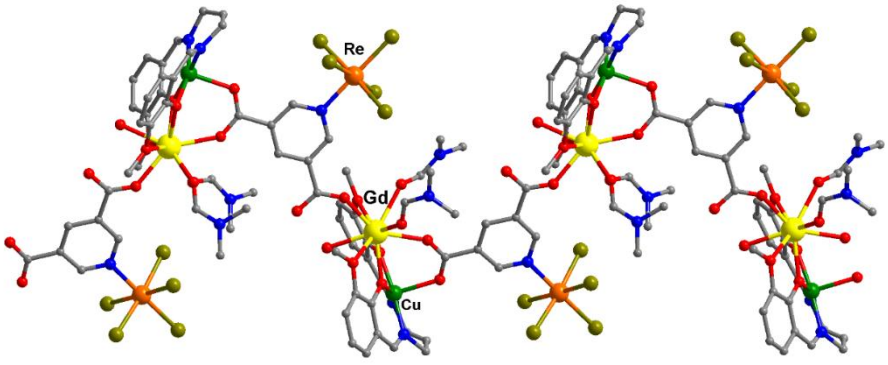

Figura 17. The structural representation of the compound $^{1}_{\infty}[\{ReBr_5(3,5\text{-pydc})\}\{Cu(valpn)Gd(H_2O)(DMF)_2\}]$ **52**.